Published in final edited form as:
Biomaterials. 2011 December ; 32(36): 9758–9765. doi:10.1016/j.biomaterials.2011.08.076.

Antibody Conjugated Magnetic Iron Oxide Nanoparticles for Cancer Cell Separation in Fresh Whole Blood

Hengyi Xu[1,2], **Zoraida P. Aguilar**[2], **Lily Yang**[3], **Min Kuang**[2], **Hongwei Duan**[4], **Yonghua Xiong**[1], **Hua Wei**[1], and **Andrew Wang**[2,*]

[1]State Key Laboratory of Food Science and Technology, Nanchang University, 235 Nanjing East Road, Nanchang 330047, P. R. China

[2]Ocean NanoTech LLC, 2143 Worth Lane, Springdale AR72764, USA

[3]Department of Surgery, Emory University School of Medicine, 1364 Clifton Road NE, Atlanta GA30322, USA

[4]Division of Bioengineering, Nanyang Technological University, 70 Nanyang Drive, Singapore 637457, Singapore

Abstract

A highly efficient process using iron oxide magnetic nanoparticles (IO)-based immunomagnetic separation of tumor cells from fresh whole blood has been developed. The process involved polymer coated 30 nm IO that was modified with antibodies (Ab) against human epithelial growth factor receptor 2 (anti-HER2 or anti-HER2/neu) forming IO-Ab. HER2 is a cell membrane protein that is over expressed in several types of human cancer cells. Using a HER2/neu over expressing human breast cancer cell line, SK-BR3, as a model cell, the IO-Ab was used to separate 73.6 % (with a maximum capture of 84%) of SK-BR3 cells that were spiked in 1 mL of fresh human whole blood. The IO-Ab preferentially bound to SK-BR3 cells over normal cells found in blood due to the high level of HER2/neu receptor on the cancer cells unlike the normal cell surfaces. The results showed that the nanosized magnetic nanoparticles exhibited an enrichment factor (cancer cells over normal cells) of 1:10,000,000 in a magnetic field (with gradient of 100 T/m) through the binding of IO-Ab on the cell surface that resulted in the preferential capture of the cancer cells. This research holds promise for efficient separation of circulating cancer cells in fresh whole blood.

Keywords

magnetic nanoparticles; iron oxide; cancer cells; cell sorting; immunomagnetic separation

INTRODUCTION

Cancer is one of the biggest public health concerns in the United States and the rest of the world. Currently, one in four deaths in the US are due to cancer and a total of 1,529,560 new

*Corresponding to, address: Ocean NanoTech LLC, 2143 Worth Lane, Springdale AR72764, USA; phone: 1-479-751-5500; fax: 1-479-751-5502; awang@oceannanotech.com. .

cancer cases with 569,490 deaths from cancer were projected in 2010 [1]. The three most commonly diagnosed types of cancer among women in 2010 were cancer of the breast, lung and bronchus, and colon/rectum; accounting for 52% of estimated cancer cases in women. Breast cancer alone is expected to account for 28% (207,090) of all new cancer cases among women; it is the most common cancer diagnosed and the second leading cause of cancer death in women in the US [1-3].

Research showed that circulating tumor cells (CTCs) can be found in patients before the primary tumor is detected [4-11]. A few CTCs may be present in peripheral blood in the background of billions of normal white blood cells (WBCs) and red blood cells (RBCs), especially during the early stage when the primary tumor is not detectable by currently available methods. In addition to a potential role in early diagnosis and prognosis, the detection of CTCs can guide therapeutic strategies for personalized treatment of patients with metastatic cancer. However, the most challenging obstacle in the separation and detection of CTCs is their extremely low concentration. Human blood normally consists of WBCs ($3\sim10\times10^{6}$ mL^{-1}), RBCs ($3\sim9\times10^{9}$ mL^{-1}), and platelets ($2.5\sim4\times10^{8}$ mL^{-1}). The number of CTCs in blood from a cancer patient may range from 0-50 mL^{-1} [12]; that is 0 to 50 CTCs in 10 billion blood cells [13]. Due to the rarity of the CTCs, existing immunomagnetic cell separation techniques lack the ability to separate the CTCs directly from whole blood [14-17].

This report is focused on the use of nanoparticles to replace the currently used micron sized magnetic beads (microbead) modified with specific antibodies that recognize the over expressed cancer cell surface protein [18]. Unlike the nanoparticles, the microbead-based magnetic separation has several limitations. First, microparticles have relatively low surface to volume ratio causing lower binding capacity and lower efficiency which is not favorable especially for tagged ligands that have low affinity constant for their receptors. Decreasing the particle sizes used in magnetic separations from micrometers to nanometers increases the available adsorptive areas by 100 to 1000 times [19]. Second, the reaction between microparticles and target cells is a quasi-heterogeneous reaction, hence, the microbeads generally takes longer time to capture the target cells in the suspensions. Third, these magnetic microbeads are not stable in whole blood forming aggregation or precipitation, thereby, leading to inefficient separation. Fourth, magnetic microbeads are generally not efficient for the separation of target cells in whole blood because of high viscosity, high cell density, high protein content, and its generally complex composition preventing efficient contact the cell surface antigen [20-22]. Furthermore, the magnetic separation of the CTCs is limited by aggregation when a large number of microbeads accumulate on the cells. Once aggregated, cell detection becomes difficult especially with flow cytometry, because the size of the aggregated cells that are captured with the microbeads affect light scattering [23]. Complicated pretreatment of blood such as dilution with buffers, centrifugation to get the buffy coat, and lysis of the RBCs, are necessary for the successful application of these magnetic microbeads [24]. These pretreatment processes can destroy the cells decreasing the cell density and at the same time, decreasing the number of CTCs making the detection more difficult. These problems and issues in magnetic-microbead based separation of CTCs may be solved with the use of nanoparticle which are three orders of magnitude smaller in size. Nanoparticles have a higher surface to volume ratio allowing a more efficient contact with the surface of the cells. The nanoscale dimensions allow multiple nanoparticles to be attached to the cell surface without cell aggregation resulting in higher magnetic susceptibility as depicted in Figure 1.

In this paper, we demonstrated the separation of circulating cancer cells using an antibody conjugated IO nanoparticles (IO-Ab) under a low magnetic field gradient. The IO nanoparticles were synthesized using pyrolysis-based method in organic solvent allowing

precise control of particle size and crystallinity. The IO nanoparticles which were soluble only in organic solvent were modified with polymers to make them water soluble before modification with the antibody that was used to capture the cancer cells. Efficiency of antibody attachment to the IO nanoparticles were investigated with gel electrophoresis while the efficiency of cell capture were monitored with Prussian blue staining and TEM. After stability evaluation, the antibody conjugated IO nanoparticles were used for cancer cell separation in buffer. We also demonstrated ability of the IO-Ab to capture cancer cells in spiked fresh human whole blood without a pre-treatment process.

Materials and Methods

Water soluble magnetic iron oxide nanoparticles

Hydrophobic IO nanoparticles were prepared using iron oxide powder as the iron precursor, oleic acid as the ligands, and octadecene as the solvent as previously described [25]. To convert the IO into biocompatible nanoparticles, these were coated with amphiphilic polymers reported previously [26]. The polymer coating provided reactive carboxyl groups on the particle surface that was used for bioconjugation. The water soluble polymer coated IO nanoparticles were purified by using a SuperMag Extra™ separator (Ocean NanoTech, Springdale, AR). The core size of the hydrophobic IO nanoparticles and the hydrophilic nanocrystal size (with the background stained with 2% phosphotungstic acid) were measured using transmission electron microscopy (TEM). The IO core nanoparticles used in this study exhibited a diameter that was approximately 30 nm.

Bioconjugation with anti-HER2 antibody

Antibody against HER2, Anti-HER2, (Herceptin, Genentech, Inc. South San Francisco, CA) was dialyzed in borate buffer and the concentration was established with a Biophotometer (Bio-rad, Philadelphia, PA). The Anti-HER2 was conjugated to the 30 nm diameter IO nanocrystal using a covalent link with the amine group ($-NH_2$) of the antibody and the carboxyl group (−COOH) of the IO nanoparticles. Briefly, the IO nanoparticles (5 mg Fe/mL) were activated by adding and incubating with sulfo-N-hydroxysuccinimide (NHS, Sigma-Aldrich, St. Louis, MO) at a molar ratio 1000:1 and 1-ethyl-3, 3-dimethylaminopropyl carbodiimide hydrochloride (EDC, Sigma-Aldrich, St. Louis, MO) at molar ratio 2000:1 for 20 minutes in borate buffer, pH 5.5, after which the pH was adjusted to 8.0. The protein, 1 mg of anti-HER2 was added immediately, mixed well, and incubated for 2 h at room temperature. The resulting antibody nanocrystal conjugates, IO-Ab, were purified using a SuperMag™ separator (Ocean NanoTech, Springdale, AR) with magnetic field gradient of 100 T/m.

The antibody conjugated IO nanoparticles were characterized with a gel electrophoresis apparatus (Bio-Rad, Hercules, CA) using 1.5% (w/v) agarose gel in Tris-acetate-EDTA (TAE) buffer, pH 8.5. For each well, 10 μL of the conjugates at 2 mg Fe/mL were mixed with 2 μL of 5×TAE loading buffer (5×TAE, 25% (v/v) glycerol at pH 8.5) before loading into the gel. The gel was resolved at 100 V for 30 min and the photo was taken with 2 s exposure using an Alpha Imager HP 2006 (Alpha Innotech, San Leandro, CA). The hydrodynamic size and the zeta potential of the IO nanoparticles before/after conjugation with the antibody were determined using Zetatrac Ultra 151 (Microtrac Inc., Montgomeryville, PA). TEM images of the IO-Ab were obtained after background staining with phosphotungstic acid.

Stability tests of the conjugates in biological fluids

The stability of IO nanoparticles with/without antibody conjugation was tested with different biological matrices including: DPBS (Invitrogen, Carlsbad, CA), DPBS + bovine serum

albumin (BSA), RPMI-1640, RPMI-1640 medium (Invitrogen, Carlsbad, CA) supplemented with 10% heat-inactivated fetal bovine serum (FBS) and 1% streptomycin/penicillin (HyClone, Logan, UT), and human plasma (ProteoGenex, Culver City, CA). Briefly, 10 μL of IO-Ab at 2 mg Fe/mL was added to 90 μL of each solution, and incubated at 37°C for 30 min. Low speed centrifugation at 3000 rpm for 5 min was applied to remove the aggregates. Agarose gel electrophoresis was used to establish possible aggregation because in a gel, aggregated nanomaterials get deposited on the wells after electrophoretic resolution. Changes in surface charge was measured with a Zetatrac Ultra 151.

Cell Culture

Human breast cancer cell line SK-BR3 which is HER2 positive was purchased from American Type Culture Collection (Rockville, MD). SK-BR3 cells were cultured in a flask containing RPMI-1640 medium supplemented with 10% heat-inactivated FBS and 1% streptomycin/penicillin. The flask was placed in a humidified atmosphere with 5% CO_2 at 37°C in a cell culture incubator (Sanyo, Japan). The media was replaced once every three days. The cells were cultured to about 80-90% confluence before harvest. During harvest, the cells were washed twice with DPBS (HyClone, Logan, UT) followed by trypsinization with 1 mL trypsin (HyClone, Logan, UT) to detach the cells from the flask. The trypsin was neutralized by adding 5 mL of fresh supplemented RPMI-1640 medium, and the harvested cells in medium suspension was transferred into a centrifuge tube and centrifuged at 250 × g for 5 min. The supernatant was discarded and the cells were resuspended in fresh medium. The cells were stained with trypan blue and inspected with a hemocytometer under an inverted microscope (Leica, Germany) to establish the cell viability and cell count.

Prussian blue staining of the IO-Ab captured SK-BR3 cells

To determine tagging of the SK-BR3 with the IO-Ab, potassium ferrocyanide and HCl staining was used. The potassium ferrocyanide and HCl mixture converts the IO from the IO-Ab accumulated on the cells into $KFe^{III}[Fe^{II}(CN)_6]$ which is blue in color.

Approximately 1×10^5 SK-BR3 cells were seeded in each well of a 6-well cell culture plate on the day before Prussian blue staining. Right before IO-Ab addition, the cells were fixed with ice-cold 95% EtOH for 15 min. This was followed by addition of IO-Ab (as 0.5 mg Fe) or IO (as 0.5 mg Fe) nanoparticles in the binding buffer (20 mM Tris, 150 mM NaCl, 2 mM $CaCl_2$, 1 mM $MnCl_2$, 1 mM $MgCl_2$, 0.1% (wt/vol) BSA; pH 7.4). The wells were incubated at room temperature for 1 h with gentle shaking. The excess reagents were removed and the cells were washed three times with DPBS buffer. Subsequently, the cells were incubated with Prussian blue staining solution (equal volumes of 20% hydrochloric acid and 10% potassium ferrocyanide aqueous solution) for 40 min at room temperature. The cells were washed twice with DPBS buffer and then placed under the microscope for inspection.

TEM of antibody-conjugated IO nanocrystal separated SK-BR3 cells

To inspect the IO-Ab + SK-BR3 capture efficiency under TEM, SK-BR3 cells were captured and separated with IO-Ab. The IO-Ab + SK-BR3 was fixed following the standard tissue fixation steps as reported [27]. The cell samples were then sliced and put on the 400 mesh copper grids for TEM.

Antibody conjugated IO nanoparticles separation of SK-BR3 cell surface protein (HER2)

To release the surface protein, SK-BR3 cell (10^6 cells) lysate was prepared using sodium dodecyl sulfate (SDS) following the standard protocol. The protein extract from the cell lysate was isolated with a Norgen protein extraction kit (Norgen Biotek Corp, Thorold, Canada) following the manufacturer's instructions. IO-Ab were used to isolate the HER2

protein from the cell lysate in the presence of a permanent magnet. A 20 uL sample of the protein extract was added to 930 μL DPBS buffer followed by 50 μL of IO-Ab (concentration expressed as 2 mg Fe/mL) and reacted at room temperature for 20 min with gentle shaking. This was incubated in Ocean's SuperMag™ separator for 1 h. The supernatant was discarded and the pellets were re-suspended in 5 μL DPBS. Carboxyl functionalized IO nanoparticles without anti-HER2/neu was similarly exposed to the protein extract as negative control.

SDS-PAGE was used to evaluate the IO-Ab capture efficiency for the HER2 protein. A Novex® Sharp pre-stained protein standard (Invitrogen, Carlsbad, CA) was used as molecular weight marker. The cell lysate, the cell whole protein extract, and IO-Ab captured protein were loaded on the SDS-PAGE and electrophoresis was carried out at 100 V for 30 min. The resulting gel was stained with Coomassie brilliant blue R25 to detect the protein bands. The gel photo was taken with 2 s exposure using an Alpha Imager HP 2006.

Cancer cell separation with IO-Ab in spiked fresh human whole blood

To establish the applicability of the IO nanoparticle mediated isolation of cells, fresh human whole blood was spiked with cancer cells. Fresh female whole blood was purchased from Biological Specialty Corporation (Colmar, PA) certified with no hepatitis or HIV contamination. The whole blood was diluted with DPBS and stained with acridine orange (AO) that stained the WBCs nuclei to pinkish yellow color without affecting the RBCs in order to establish the number of WBCs and RBCs. Briefly 10 μL of whole blood was diluted at 1:100 with DPBS and mixed with the AO at a ratio of 1:1. The mixture was incubated for 10 min at room temperature; the cells were pelleted by centrifugation at 5,000 rpm for 5 min. Excess AO was washed with DPBS two times. The AO stained cells were counted using a hemocytometer under a fluorescence microscope. All the experiments involving human blood were performed in a BSL2 laboratory.

Cultured SK-BR3 cells were pre-stained with a live cell staining fluorescent dye CMFDA (Invitrogen, Carlsbad, CA) that converted the cells to green color following the manufacture's staining protocol. The cells were counted and spiked in 1 mL whole blood sample. A 0.05 mL of IO-Ab nanoparticles at a concentration expressed as 2 mg Fe/mL was added to the SK-BR3 spiked whole blood and mixed gently at room temperature for 1 h to form IO-Ab + cells. The mixture was placed on a SuperMag™ separator for 1 h to allow magnetic isolation of the IO-Ab + cells. The supernatant fluid was gently withdrawn with a pipettor making sure not to disturb the captured IO-Ab + cells that stuck on the wall of the tube where the magnetic field was strongest. The captured pellet containing the IO-Ab + cells were re-suspended in 100 μL DPBS for cell inspection and counting.

Statistical analyses

The data gathered were analyzed using the statistical program SigmaPlot 8.02 (SPSS, Inc., Chicago, USA). All the tests were performed at least in duplicate.

Results and discussion

Characterizations of IO nanoparticles

Initially, the IO nanoparticles were synthesized using a modified pyrolysis-based method in organic solvent [25]. These IO nanoparticles were spherical, hydrophobic, highly ordered Fe_3O_4 crystals, with an average inorganic core diameter of 27±5 nm (relative standard deviation of 9.5% for n=50) as shown in Figure 2A. These hydrophobic core IO nanoparticles were converted into the biocompatible water soluble form with the use of amphiphilic polymer that interacted with the original hydrophobic oleate coating resulting in

a double layered structure with carboxyl groups on the surface. The functionalization led to 6 nm in total extra thickness that resulted in an average hydrodynamic size of 33 nm in aqueous suspension (Figure 2C). When the IO nanoparticles were conjugated with anti-HER2, the particle size and surface charge increased as a result of the 2-4 nm diameter antibody. The antibody attachment on the IO surface was manifested in the phosphotungstic acid background stained TEM (Figure 2B), presenting a thicker layer compared with the TEM of the IO inorganic core alone (Figure 2A). As shown in Figure 2C, the hydrodynamic size of IO-Ab nanoparticles was 41 nm showing an increase of about 8 nm in diameter. In addition, after the antibody conjugation, a decrease in zeta potential from −51 mV to −36 mV was also observed.

As shown in Figure 2D, the migration of the IO-Ab in agarose gel towards the positive pole was much slower than the IO without the Ab. This may be attributed to the bigger and higher molecular weight IO-Ab with a less negative zeta potential. The less negative zeta potential may be attributed to the surface charge shielding of the carboxyl groups after these were reacted with the amine groups on the antibodies. The increase in size may be attributed to the conjugation of the antibodies plus the water of hydration on the conjugate surface.

Stability in biological fluids

The most common problem for biological applications of nanomaterials is their compatibility with various biological conditions of temperature, pH, salinity, viscosity, toxicity, and many more [28-30]. Some engineered nanomaterials release heavy metal ions and cause harm to biological samples because of their instability in biological conditions [31]. Other nanoparticles are not stable in biological fluids hindering their biological applications [32]. Thus, we tested the stability and compatibility of our IO nanoparticles and their conjugates in different biological buffers and fluids. As shown in Figure 3, antibody conjugated IO were stable in all the biological buffers/fluids tested whereas, carboxyl functionalized IO showed severe precipitation in RPMI-1640 medium (these test were repeated twice). Thus, it was necessary for the cells to be removed from RPMI-1640 medium when exposed to the IO-Ab conjugates.

Antibody-conjugated IO nanocrystal separation of SK-BR3 cells in buffer

When antibodies are conjugated to a molecule, there is always the possibility that the binding affinity and binding efficiency may be affected. It is also possible that binding from the molecular to cellular level can be changed because of the size of the cell membrane as well as non-specific binding of the IO nanoparticles.

In order to study the affinity and specificity of the IO-Ab mediated protein capture forming IO-Ab+HER2, Prussian blue staining was used to exhibit specific attachment to the cell surface. The Prussian blue concept was based on the formation of blue coloration in the presence of Fe ions. As shown in Figure 4A, cells that were specifically labeled with IO-Ab showed very significant dark blue coloration, whereas the carboxyl functionalized IO without anti-HER2 antibody that were non-specifically bound to the cells showed less blue coloration (Figure 4B). Thus, the amount of non-specifically attached IO on the cell membrane was insignificant compared with the amount of attached IO-Ab. The Prussian blue staining confirmed specific binding of the IO-Ab on the targeted cells that were isolated with a permanent magnet.

Additionally, the evidence of the presence of IO on the cell surface was confirmed by TEM. As shown in Figure 4C and 4D, IO nanoparticles were found on the cell membranes which may be attributed to the specific targeting with the conjugated anti-HER2/neu. The high density of IO on the cell membrane indicated that small sized nanoparticles were highly

efficient in targeting the cells which allowed ease of separation without cell membrane damage preserving the integrity of the cells. However, cellular uptake of the IO-Ab were observed under TEM, as shown in Figure 4E, where cellular vesicles were found to contain IO. The endocytotic pathway is usually the main mechanism for cell ingestion of extracellular substances, which can further be confined inside endosomes and digested by enzymes to protect the cell itself. Compared with the number of particles specifically attached on the cell surface, the intracellular cell uptake of the IO was insignificant.

Antibody conjugated IO nanoparticles separation of SK-BR3 cell surface protein (HER2)

HER2 is a cell membrane surface-bound protein receptor tyrosine kinase and is normally involved in the signal transduction pathways leading to cell growth and differentiation [33]. HER2/neu is over expressed in 20 to 30% of human breast cancer tissues as well as several other tumor types [34, 35]. In this study, we extracted the whole surface protein from SK-BR3 cells and selectively concentrated the HER2 protein with IO-Ab. As shown in the SDS PAGE results in Figure 5, HER2 protein was selectively captured with the IO-Ab based on the retarded migration of the IO-Ab on Lanes 5, 6, and 7 in comparison with the original cell lysate shown on Lane 2 or the whole protein extract on Lane 3. HER2 was not captured with carboxyl functionalized IO without the conjugated anti-HER2 (Lane 4). These results indicated that capture and enrichment of the HER2 was achieved only when IO was conjugated with the specific antibody.

It was previously reported that SK-BR3 cells express as much as 1×10^6 to 2.6×10^6 HER2 receptors per cell, whereas the normal cells express only 2×10^4 HER2 receptors per cell [36-38]. Used as a target protein, the HER2 cell membrane surface proteins are good candidates for whole cancer cell capture and separation using the IO-Ab. This difference in the number of HER2 receptors between SK-BR3 cell and white blood cell was used to demonstrate the application of magnetic IO nanoparticles for efficient targeted cell separation and enrichment from whole blood.

Cancer cell separation with antibody conjugated IO nanoparticles in whole blood

To demonstrate the effectiveness of IO-Ab to capture CTCs in whole blood, we used SK-BR3 cells spiked in fresh human whole blood. The results are shown in Figure 6. To generate this data, the number of white blood cells in commercial female whole blood was counted at 4.2×10^7 cells/mL and the red blood cells at 4.4×10^9 cells/mL. During the cancer cell separation process, 300 of the CMFDA pre-stained SK-BR3 cells (Figure 6A) were added to 1 mL whole blood with a ratio of cancer cells to blood cells (WBCs and RBCs) at about 1:10,000,000. The spiked whole blood was exposed to the IO-Ab to allow formation of the IO-Ab + SK-BR3 captured cells. The IO-Ab + SK-BR3 captured cells were resuspended in 100 μL DPBS, smeared on a clean microscope glass slide, inspected, and counted under a microscope. The CMFDA stained SK-BR3 cells appeared greenish yellow in color which were bigger in diameter than the WBCs and RBCs. As shown in Figure 6B, the SK-BR3 cells were successfully captured directly from spiked fresh human whole blood. The recovery was as high as 86% with 73.6% in average (N=5) in an unoptimized system, which was 23.5% better than that reported for magnetic microparticles [39-41]. An enrichment factor of 1:10,000,000 were attained based on the number of WBCs and RBCs in the spiked whole blood using our 30 nm diameter iron oxide nanoparticles in the presence of a low magnetic field gradient. The increased cell enrichment was attributed to the 30 nm diameter magnetic nanoparticles that allowed for greater number of particles to attach on the cell surface. The unique features of these hydrophilic biocompatible polymer coated iron oxide nanoparticles with high mobility, stronger binding ability, and high colloidal stability in whole blood contributed to the high enrichment factor. The system developed for

isolation of specific cells using IO nanoparticles that are conjugated to specific antibodies holds promise for the isolation and enrichment of CTCs in fresh human whole blood.

Conclusion

We demonstrated a highly efficient process using iron oxide magnetic nanoparticles for the capture and separation of tumor cells from fresh whole blood. The process involved polymer coated 30 nm IO that was modified with antibodies against human epithelial growth factor receptor 2 (anti-HER2 or anti-HER2/neu) forming IO-Ab. Using a HER2/neu over expressing human breast cancer cell line, SK-BR3, as a cell model system, the IO-Ab was used to separate 73.6 % (N=5, with a maximum enrichment of 84%) of SK-BR3 cells that were spiked in 1 mL of fresh human whole blood. The IO-Ab preferentially bound with SK-BR3 cells over normal cells found in blood due to the high level of HER2/neu receptor on the cancer cell surfaces. The results showed that the nanosized iron oxide magnetic nanoparticles successfully exhibited 1:10,000,000 enrichment of cancer cells over normal cells in the presence of a magnetic field gradient of 100 T/m.

Acknowledgments

This work was partly supported by a grant from National Institute of Health (NIH, grant # 1 R43 CA134066) and National Science Foundation (NSF, grant #0810626). This work was also supported in part by a grant from “Cultivating the Excellent Ph. D Thesis of Jiangxi Province (YBP08A03)” of the Education Department of Jiangxi Province, China. The authors would like to thank Mr. Benjamin Jones for the picture drawing and Mr. John Dixon for purification of the IO nanoparticles; University of Arkansas’s REU students Joy Labayan, Chong Thor, and Debby Chou for cell counting and picture taking.

References

[1]. Jemal A, Siegel R, Xu J, Ward E. Cancer statistics, 2010. CA Cancer J Clin. 2010; 60:277–300. [PubMed: 20610543]

[2]. Jemal A, Siegel R, Ward E, Hao Y, Xu J, Murray T, et al. Cancer Statistics, 2008. CA Cancer J Clin. 2008; 58:71–96. [PubMed: 18287387]

[3]. Jemal A, Siegel R, Ward E, Hao Y, Xu J, Thun M. Cancer statistics, 2009. CA Cancer J Clin. 2009; 59:225–49. [PubMed: 19474385]

[4]. Ghossein R, Bhattacharya S, Rosai J. Molecular detection of micrometastases and circulating tumor cells in solid tumors. Clin Cancer Res. 1999; 5:1950–60. [PubMed: 10473071]

[5]. Gaforio JJ, Serrano MJ, Sanchez-Rovira P, Sirvent A, Delgado-Rodriguez M, Campos M, et al. Detection of breast cancer cells in the peripheral blood is positively correlated with estrogen-receptor status and predicts for poor prognosis. Int J Cancer. 2003; 107:984–90. [PubMed: 14601059]

[6]. Molnar B, Ladanyi A, Tanko L, Sréter L, Tulassay Z. Circulating tumor cell clusters in the peripheral blood of colorectal cancer patients. Clin Cancer Res. 2001; 7:4080–5. [PubMed: 11751505]

[7]. Méhes G, Witt A, Kubista E, Ambros PF. Circulating breast cancer cells are frequently apoptotic. Am J Pathol. 2001; 159:17–20. [PubMed: 11438448]

[8]. Meng S, Tripathy D, Frenkel EP, Shete S, Naftalis EZ, Huth JF, et al. Circulating tumor cells in patients with breast cancer dormancy. Clin Cancer Res. 2004; 10:8152–62. [PubMed: 15623589]

[9]. Pierga JY, Bonneton C, Vincent-Salomon A, de Cremoux P, Nos C, Blin N, et al. Clinical significance of immunocytochemical detection of tumor cells using digital microscopy in peripheral blood and bone marrow of breast cancer patients. Clin Cancer Res. 2004; 10:1392–400. [PubMed: 14977842]

[10]. Hayes DF, Walker TM, Singh B, Vitetta ES, Uhr JW, Gross S, et al. Monitoring expression of HER-2 on circulating epithelial cells in patients with advanced breast cancer. Int J Oncol. 2002; 21:1111–7. [PubMed: 12370762]

[11]. O'Hara SM, Moreno JG, Zweitzig DR, Gross S, Gomella LG, Terstappen LW. Multigene reverse transcription-PCR profiling of circulating tumor cells in hormone-refractory prostate cancer. Clin Chem. 2004; 50:826–35. [PubMed: 14988224]

[12]. Allard WJ, Matera J, Miller MC, Repollet M, Connelly MC, Rao C, et al. Tumor cells circulate in the peripheral blood of all major carcinomas but not in healthy subjects or patients with nonmalignant diseases. Clin Cancer Res. 2004; 10:6897–904. [PubMed: 15501967]

[13]. Liberti PA, Rao CG, Terstappen LW. Optimization of ferrofluids and protocols for the enrichment of breast tumor cells in blood. J Magn Magn Mater. 2001; 225:301–7.

[14]. Berois N, Varangot M, Osinaga E, Babino A, Caignault L, Musé I, et al. Detection of rare human breast cancer cells. Comparison of an immunomagnetic separation method with immunocytochemistry and RT-PCR. Anticancer Res. 1997; 17:2639–46. [PubMed: 9252694]

[15]. Berry CC, Wells S, Charles S, Curtis AS. Dextran and albumin derivatised iron oxide nanoparticles: influence on fibroblasts *in vitro*. Biomaterials. 2003; 24:4551–7. [PubMed: 12950997]

[16]. Mapara MY, Körner IJ, Hildebrandt M, Bargou R, Krahl D, Reichardt P, et al. Monitoring of tumor cell purging after highly efficient immunomagnetic selection of CD34 cells from leukapheresis products in breast cancer patients: comparison of immunocytochemical tumor cell staining and reverse transcriptase-polymerase chain reaction. Blood. 1997; 89:337–44. [PubMed: 8978310]

[17]. Molday RS, MacKenzie D. Immunospecific ferromagnetic iron-dextran reagents for the labeling and magnetic separation of cells. J Immunol Methods. 1982; 52:353–67. [PubMed: 7130710]

[18]. Miltenyi S, Müller W, Weichel W, Radbruch A. High gradient magnetic cell separation with MACS. Cytometry. 1990; 11:231–8. [PubMed: 1690625]

[19]. Yavuz CT, Mayo JT, Yu WW, Prakash A, Falkner JC, Yean S, et al. Low-field magnetic separation of monodisperse Fe_3O_4 nanocrystals. Science. 2006; 314:964–7. [PubMed: 17095696]

[20]. Martin VM, Siewert C, Scharl A, Harms T, Heinze R, Ohl S, et al. Immunomagnetic enrichment of disseminated epithelial tumor cells from peripheral blood by MACS. Exp Hematol. 1998; 26:252–64. [PubMed: 9502622]

[21]. Safarík I, Safaríková M. Use of magnetic techniques for the isolation of cells. J Chromatogr B Biomed Sci Appl. 1999; 722:33–53. [PubMed: 10068132]

[22]. Pamme N, Wilhelm C. Continuous sorting of magnetic cells via on-chip free-flow magnetophoresis. Lab Chip. 2006; 6:974–80. [PubMed: 16874365]

[23]. Xu, R. Particle characterization: light scattering methods. Kluwer Academic Publishers; Dordrecht: 2001. p. 223-83.

[24]. Tong X, Yang L, Lang JC, Zborowski M, Chalmers JJ. Application of immunomagnetic cell enrichment in combination with RT-PCR for the detection of rare circulating head and neck tumor cells in human peripheral blood. Cytometry B Clin Cytom. 2007; 72:310–23. [PubMed: 17205568]

[25]. Yu WW, Falkner JC, Yavuz CT, Colvin VL. Synthesis of monodisperse iron oxide nanocrystals by thermal decomposition of iron carboxylate salts. Chem Commun (Camb). 2004:2306–7. [PubMed: 15489993]

[26]. Gao X, Cui Y, Levenson RM, Chung LW, Nie S. *In vivo* cancer targeting and imaging with semiconductor quantum dots. Nat Biotechnol. 2004; 22:969–76. [PubMed: 15258594]

[27]. Chithrani BD, Ghazani AA, Chan WC. Determining the size and shape dependence of gold nanoparticle uptake into mammalian cells. Nano Lett. 2006; 6:662–8. [PubMed: 16608261]

[28]. Yu S, Chow GM. Carboxyl group ($-CO_2H$) functionalized ferrimagnetic iron oxide nanoparticles for potential bio-applications. J Mater Chem. 2004; 14:2781–6.

[29]. Majewski P, Thierry B. Functionalized magnetite nanoparticles--synthesis, properties, and bio-applications. Crit Rev Solid State Mater Sci. 2007; 32:203–15.

[30]. Hirsch LR, Jackson JB, Lee A, Halas NJ, West JL. A whole blood immunoassay using gold nanoshells. Anal Chem. 2003; 75:2377–81. [PubMed: 12918980]

[31]. Derfus AM, Chan WC, Bhatia SN. Probing the cytotoxicity of semiconductor quantum dots. Nano Lett. 2004; 4:11–8.

[32]. Smith AM, Duan H, Rhyner MN, Ruan G, Nie S. A systematic examination of surface coatings on the optical and chemical properties of semiconductor quantum dots. Phys Chem Chem Phys. 2006; 8:3895–903. [PubMed: 19817050]

[33]. Reese DM, Slamon DJ. HER-2/neu signal transduction in human breast and ovarian cancer. Stem cells. 1997; 15:1–8. [PubMed: 9007217]

[34]. Grushko, TA.; Olopade, OI. Genetic markers in breast tumors with hereditary predisposition. In: Bronchud, MH.; Foote, MA.; Giaccone, G.; Olopade, O.; Workman, P., editors. Principles of molecular oncology. Humana press; Totowa: 2008. p. 85-105.

[35]. Disis ML, Goodell V, Schiffman K, Knutson KL. Humoral epitope-spreading following immunization with a HER-2/neu peptide based vaccine in cancer patients. J Clin Immunol. 2004; 24:571–8. [PubMed: 15359116]

[36]. Sarup JC, Johnson RM, King KL, Fendly BM, Lipari MT, Napier MA, et al. Characterization of an anti-p185HER2 monoclonal antibody that stimulates receptor function and inhibits tumor cell growth. Growth Regul. 1991; 1:72–82. [PubMed: 1688187]

[37]. Lewis GD, Figari I, Fendly B, Wong WL, Carter P, Gorman C, et al. Differential responses of human tumor cell lines to anti-p185HER2 monoclonal antibodies. Cancer Immunol Immunother. 1993; 37:255–63. [PubMed: 8102322]

[38]. Lee J, Dull TJ, Lax I, Schlessinger J, Ullrich A. HER2 cytoplasmic domain generates normal mitogenic and transforming signals in a chimeric receptor. EMBO J. 1989; 8:167–73. [PubMed: 2565808]

[39]. Inglis DW, Riehn RR, Austin RH, Sturm JC. Continuous microfluidic immunomagnetic cell separation. Appl Phys Lett. 2004; 85:5093.

[40]. Zborowski M, Sun L, Moore LR, Williams PS, Chalmers JJ. Continuous cell separation using novel magnetic quadrupole flow sorter. J Magn Magn Mater. 1999; 194:224–30.

[41]. von Schönfeldt V, Krishnamurthy H, Foppiani L, Schlatt S. Magnetic cell sorting is a fast and effective method of enriching viable spermatogonia from Djungarian hamster, mouse, and marmoset monkey testes. Biol Reprod. 1999; 61:582–9. [PubMed: 10456832]

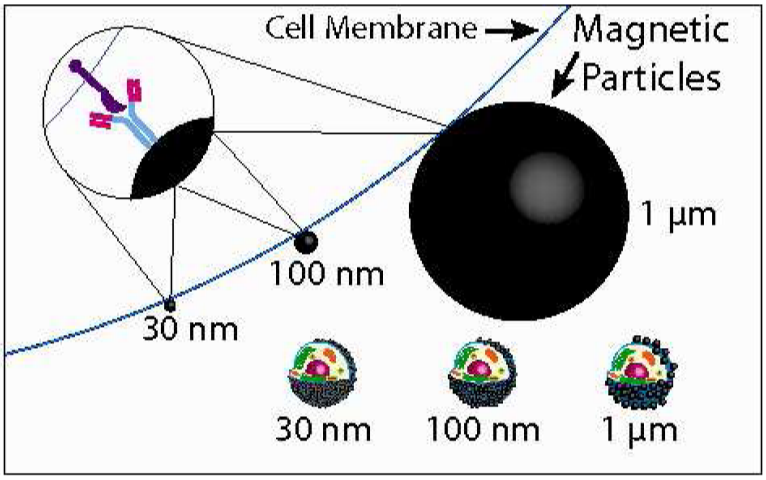

Figure 1.
Schematic diagram of immunomagnetically labeled cell with particles of different diameters. The number of nanosize particles that can be attached on the cell surface is higher than the microsize particles because of less steric exclusion.

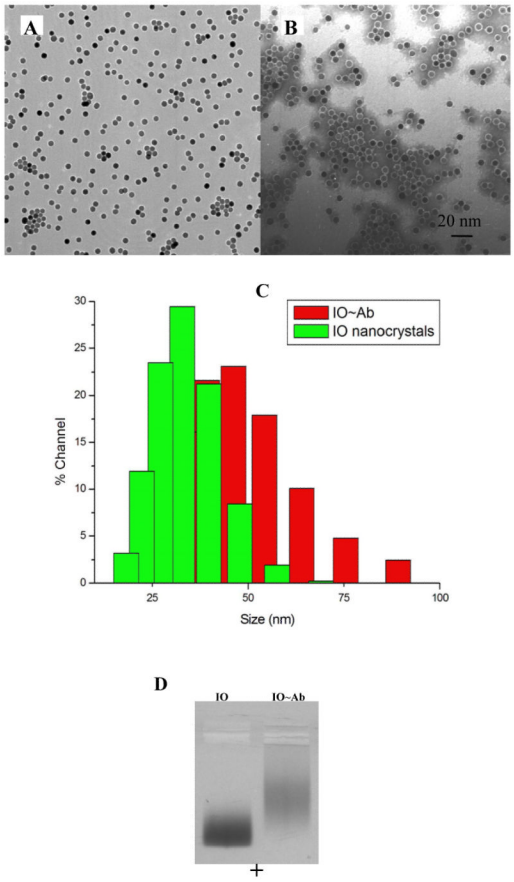

Figure 2.

Characterization of IO nanoparticles. A) TEM image of the hydrophobic inorganic core of the IO nanoparticles, showing a diameter around 27±5 nm (relative standard deviation of 9.5% for *n*=50); B) TEM image of antibody conjugated biocompatible water soluble IO, IO-Ab, using phosphotungstic acid for background staining; C) light scattering properties of biocompatible water soluble IO showing a hydrodynamic size around 33 nm with a zeta potential of −51mV, and IO-Ab showing a hydrodynamic size around 41 nm and a zeta potential of −36 mV; D) agarose gel electrophoresis of biocompatible water soluble IO (on left) and IO-Ab (on right), the electric pole is negative for top and positive for the bottom.

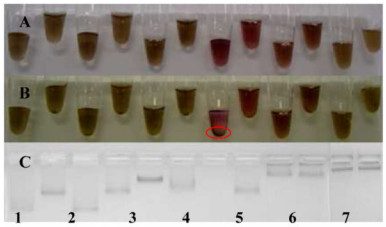

Figure 3.

Stability test of antibody conjugated IO nanoparticles in biological fluids: 1) carboxyl functionalized IO nanoparticles control in DDW, 2) IO-Ab nanoparticles control in DDW, 3) carboxyl functionalized IO nanoparticles in DPBS, 4) IO-Ab nanoparticles in DPBS, 5) carboxyl functionalized IO nanoparticles in DPBS+1% (w/v) BSA, 6) IO-Ab nanoparticles in DPBS+1% (w/v) BSA, 7) carboxyl functionalized IO nanoparticles in RPMI-1640, 8) IO-Ab nanoparticles in RPMI-1640, 9) carboxyl functionalized IO nanoparticles in RPMI-1640 supplemented with 10% heat-inactivated FBS and 1% streptomycin/penicillin, 10) IO-Ab nanoparticles in RPMI-1640 supplemented with 10% heat-inactivated FBS and 1% streptomycin/penicillin, 11) carboxyl functionalized IO nanoparticles in human plasma, and 12) IO-Ab nanoparticles in human plasma. A) before centrifugation, B) after centrifugation at 3000 rpm for 5 min, and C) agarose gel electrophoresis.

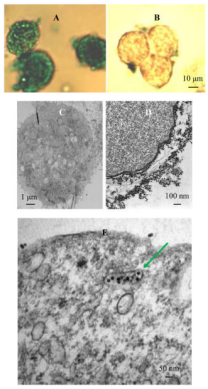

Figure 4.

Cell staining with Prussian blue. SK-BR3 cells A) exposed to IO-Ab, B) exposed to carboxyl functionalized IO; TEM of IO-Ab targeted C) whole cell section under low magnifications, D) partially magnified cell membrane exposed to IO-Ab; and E) IO-Ab taken up by the cell.

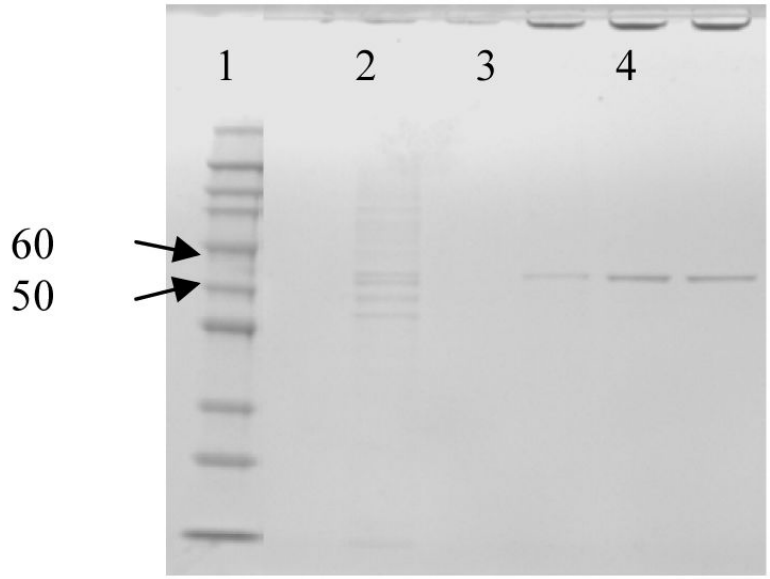

Figure 5.
SDS-PAGE of HER2 from SK-BR3 cell lysate . Lane 1: Marker; Lane 2: 10^6 SK-BR3 cell lysate; Lane 3: whole protein extract using Norgen kit; Lane 4: control- carboxyl functionalized IO for capture; Lane 5: IO-Ab for capturefrom non-purified SK-BR3 cell lysate; Lane 6: IO-Ab capture from purified whole protein extracted from 10^5 SK-BR3; and Lane 7: IO-Ab captured HER2 from purified whole protein extracted from 10^6 SK-BR3.

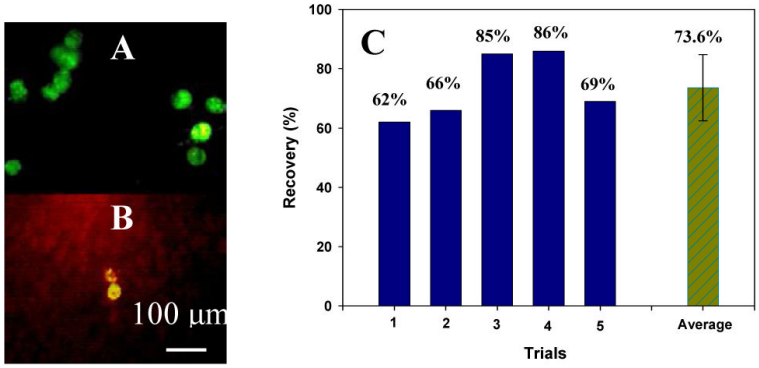

Figure 6.

SK-BR3 cell separation in spiked female whole blood. A) SK-BR3 cell pre-stained with CMFDA, B) isolated CMFDA pre-stained SK-BR3 cells from whole blood, C) IO-Ab captured cell from spiked whole blood.